

## RESEARCH ARTICLE

# Sticky, stickier and stickiest – a comparison of adhesive performance in clingfish, lumpfishes and snailfish

Jonathan M. Huie<sup>1,\*†</sup>, Dylan K. Wainwright<sup>2,3,\*</sup>, Adam P. Summers<sup>4,5</sup> and Karly E. Cohen<sup>4,5,6</sup>

## ABSTRACT

The coastal waters of the North Pacific are home to the northern clingfish (*Gobiesox maeandricus*), Pacific spiny lumpfisher (*Eumicrotremus orbis*) and marbled snailfish (*Liparis dennyi*) – three fishes that have evolved ventral adhesive discs. Clingfish adhesive performance has been studied extensively, but relatively little is known about the performance of other sticky fishes. Here, we compared the peak adhesive forces and work to detachment of clingfish, lumpfishes and snailfish on surfaces of varying roughness and over ontogeny. We also investigated the morphology of their adhesive discs through micro-computed tomography scanning and scanning electron microscopy. We found evidence that adhesive performance is tied to the intensity and variability of flow regimes in the fishes' habitats. The northern clingfish generates the highest adhesive forces and lives in the rocky intertidal zone where it must resist exposure to crashing waves. Lumpfishes and snailfish both generate only a fraction of the clingfish's adhesive force, but live more subtidal where currents are slower and less variable. However, lumpfishes generate more adhesive force relative to their body weight than snailfish, which we attribute to their higher-drag body shape and frequent bouts into the intertidal zone. Even so, the performance and morphology data suggest that snailfish adhesive discs are stiffer and built more efficiently than lumpfisher discs. Future studies should focus on sampling additional diversity and designing more ecologically relevant experiments when investigating differences in adhesive performance.

**KEY WORDS:** Suction, Flow, Fluorescence, Ecology, Pelvic disc, Work

## INTRODUCTION

Many fishes have independently evolved diverse strategies and morphologies for adhering to surfaces using suction-based adhesion. Clingfishes (Gobiesocidae), gobies (Gobiidae), lumpfishes (Cyclopteridae) and snailfishes (Liparidae) have a ventral adhesive disc supported by the pelvic, or pectoral and pelvic girdles (Arita, 1967; Budney and Hall, 2010; Wainwright et al., 2013; Maie and Blob, 2021; Palecek et al., 2021a). Remoras

(Echeneidae) have a dorsal adhesive disc made from modified dorsal fins, suckermouth catfishes (Loricariidae) and lampreys (Petromyzontiformes) have oral suckers, and hillstream loaches (Balitoridae) generate suction using their whole body (De Meyer and Geerinckx, 2014; Wang et al., 2017; Willis et al., 2019 preprint; Bressman et al., 2020; Cohen et al., 2020a,b; Wang et al., 2020; Shi et al., 2021). Suction-based adhesion likely evolved as an adaptation for resisting high-flow environments (e.g. crashing waves in the intertidal zone or fast-flowing streams), but suctorial organs have been co-opted for locomotion or feeding (Lujan and Conway, 2015). Island gobies use them to climb waterfalls, remoras hitch a ride aboard larger fauna, and clingfish use their disc to launch predatory attacks on limpets. Despite the broad ecological and morphological diversity of fishes with adhesive discs, there is surprisingly little comparative data on their adhesive abilities.

Many studies testing the limits of ventral adhesive discs have focused on the northern clingfish [*Gobiesox maeandricus* (Girard 1858)]. It is a rocky intertidal specialist from the North Pacific Ocean that uses a large adhesive disc to attach to rocks and resist high-energy waves (Ditsche et al., 2017). The northern clingfish can generate adhesive forces up to 250 times its body weight and adhere to a wide range of challenging substrates including rough, compliant and fouled surfaces covered in algae and biofilm (Wainwright et al., 2013; Ditsche et al., 2014; Huie and Summers, 2022). Biomimetic suction cups based on clingfish reveal the key components needed for a successful disc that can operate in diverse conditions. The soft margin of the adhesive disc forms a tight seal on rough surfaces by matching the surface's irregularities, while the bony support from the pelvic and pectoral girdles prevents the disc from collapsing in on itself (Ditsche and Summers, 2019; Sandoval et al., 2019). The contact surface of the disc has papillae, small hierarchical pads that terminate in hair-like features, that putatively improve suction by increasing friction between the disc and substrate (Wainwright et al., 2013; Ditsche and Summers, 2019; Sandoval et al., 2020).

Living alongside the northern clingfish, but in different habitats, are the Pacific spiny lumpfisher [*Eumicrotremus orbis* (Günther 1861)] and marbled snailfish (*Liparis dennyi* Jordan & Starks 1895). Pacific spiny lumpfishes are small, heavily armored fish that live in both intertidal and subtidal environments, but always remain submerged (depth 0–575 m) (Arita, 1969; Kells et al., 2016; Woodruff et al., 2022). Their rotund body shape makes them slow swimmers and susceptible to high drag forces, but they have a relatively large ventral suction disc for adhering to rocks and barnacles (Arita, 1967). The marbled snailfish is an elongate, subtidal species (depth 73–225 m), with a relatively small adhesive disc (Pietsch and Orr, 2015). Recent phylogenetic reconstructions suggest that lumpfishes and snailfish inherited their adhesive discs from a shared common ancestor, suggesting that their disc morphologies and performance may be relatively similar (Gerringer et al., 2021). However it is unknown how much the adhesive performance of these species differs, or how they compare to the

<sup>1</sup>Department of Biological Sciences, The George Washington University, Washington, DC 20052, USA. <sup>2</sup>Department of Biology, Purdue University, West Lafayette, IN 47907, USA. <sup>3</sup>Department of Forestry and Natural Resources, Purdue University, West Lafayette, IN 47907, USA. <sup>4</sup>Friday Harbor Laboratories, University of Washington, Friday Harbor, WA 98250, USA. <sup>5</sup>Department of Biology, University of Washington, Seattle, WA 98195, USA. <sup>6</sup>Department of Biology, University of Florida, Gainesville, FL 32611, USA.

\*Co-first authorship

†Author for correspondence (jonathanmhuie@gmail.com)

J.M.H., 0000-0002-7925-7372; D.K.W., 0000-0003-4964-5048; A.P.S., 0000-0003-1930-9748; K.E.C., 0000-0001-6556-5414

Received 28 July 2022; Accepted 28 October 2022

northern clingfish. These three species provide an opportune system to assess the relationship between ecology and adhesive performance because in the Pacific Northwest, they are geographically sympatric but prefer different habitats. Clingfish must brace themselves against crashing waves and exposure to gravity during low tides, whereas lumpfish and snailfish live at depths where ocean currents are slower and less variable (Holbrook, 1980). Unlike the marbled snailfish that is restricted to subtidal depths, spiny lumpfish are also found in deep tidepools or nearshore, where they experience more intense and varied flow regimes. We hypothesize that the adhesive performance of these three species will reflect the intensity and variability of flow in their respective habitats, as evidence of evolutionary tuning between performance and environmental demands (Maie et al., 2012; Palecek et al., 2021a).

The amount of force and work needed to detach an adhesive disc are two ways to measure adhesive performance. Peak adhesive force (also called pull-off force or force to failure) is a classic measurement for investigating the performance of biological and manufactured suction cups, because it indicates how strong the adhesion is, as well as how much weight the suction cup can support (Fulcher and Motta, 2006; Wainwright et al., 2013; Wang et al., 2017; Christy and Maie, 2019; Ditsche and Summers, 2019; Gamel et al., 2019; Maie and Blob, 2021; Sandoval et al., 2019). Work, also called work to detachment or failure, represents a biologically relevant concept – the amount of energy needed to detach the fish from its substrate. While peak force is an instantaneous measurement, total work – measured as the area under a force–extension curve – integrates more information and is independent of the detachment force. It is possible that peak force and work may reveal similar patterns in relative performance if the shapes of the force–extension curves are consistent. However, clingfish that had lower adhesive forces on soft material still required the same amount of energy to be detached as they did on stiffer substrates (Huie and Summers, 2022). It is not clear which variable is more relevant in biological scenarios, but they capture different information and, therefore, both are valuable for understanding whole-organism performance.

In aquatic environments, drag forces due to water flow are a major factor acting to displace lumpfish, snailfish and clingfish. Drag scales with the area of an object's profile; thus, bigger fishes experience larger drag forces than smaller fishes. As a result, we should expect adhesive performance to scale proportionally over ontogeny in predictable ways. Deviations from these expected patterns may indicate either that the effects of drag are changing over ontogeny (e.g. due to changes in body shape, habitat or behavior) or that the relative importance of adhesive performance changes. To alter adhesive performance, natural selection may act on the relative size and shape of the adhesive discs. Adhesive disc area is a strong predictor of suction forces, but additional morphological differences in the bony supports and soft tissue may also contribute to differences in performance (Palecek et al., 2022). In this study, we generated adhesion data for the Pacific spiny lumpfish (*E. orbis*) and the marbled snailfish (*L. dennyi*), and compared these with published data for the northern clingfish (*G. maeandricus*; Wainwright et al., 2013). Our goals were threefold: (1) to compare differences in adhesive performance on surfaces of varying roughness, (2) to assess differences in the relationship between size and adhesive performance, and (3) to compare hard and soft tissues of the discs of all three species. By comparing these three North Pacific species living at different depths with varied flow regimes, we hope to better understand the extent to which adhesive performance varies with lineage, size and ecology.

## MATERIALS AND METHODS

### Animals

Pacific spiny lumpfish and marbled snailfish were collected near San Juan Island, WA, USA. In 2013, snailfish [ $n=12$ , standard length (SL) 9.8–14.8 cm] were collected off-shore with an otter trawl at a depth of around 100 m. In 2021, lumpfish [ $n=7$ , SL 2.5–6.2 cm, body mass (BM) 2.7–17.8 g] were collected at night off the docks of Friday Harbor Laboratories, WA, USA, with a fishing light and a dip net. Animals were tested in the same year they were caught and housed in a flow-through tank system prior to adhesion testing. Immediately before testing, specimens were euthanized with MS-222, weighed (lumpfish only) and photographed. We used FIJI (Schindelin et al., 2012) to digitally measure SL and the area of the adhesive disc for each specimen.

Cohen and Summers (2022) showed that the adhesive discs (specifically the papillae) of the Pacific spiny lumpfish fluoresce. In 2021, we collected new clingfish ( $n=5$ , SL 6.5–8.0 cm) and snailfish ( $n=2$ , SL 12.7 and 14.2 cm) specimens to determine whether these species also fluoresce when exposed to royal blue (440–460 nm) light (NIGHTSEA™). The sexes of these specimens were unknown, except for the smaller snailfish specimen, which was a gravid female. None of these specimens were used for adhesion testing. All procedures in this study were approved by an Institutional Animal Care and Use Committee protocol at Friday Harbor Laboratories.

Some of our statistical analyses required the use of body mass, but these data were not collected for the snailfish specimens. Therefore, we estimated their mass using published length–mass relationships for *Liparis pulchellus* and *Liparis ochotensis*, two closely related snailfish species, as well as the estimated marbled snailfish length–mass relationship on FishBase (Johnson, 1969; Froese et al., 2014; Kulik and Gerasimov, 2016). The results of our interspecific comparisons and scaling analyses were qualitatively similar, regardless of the length–mass relationship that was used. Here, we report the results that used the *L. pulchellus* length–mass relationship, and include additional mass-dependent results in Table S4.

### Measuring suction performance

We measured the adhesive forces of each specimen on six different surfaces of varying roughness, following the procedure outlined in Wainwright et al. (2013). Substrates were generated by casting epoxy resin into molds made from glass and five kinds of sandpaper (Buehler CarbiMet™ 2; P1200, P400, P280, P180 and P120, matching average grit sizes of 15.3, 35, 52, 78 and 127 µm, respectively). The substrates were then glued to the bottom of watertight containers. We measured the adhesive forces of each fish using an MTS Synergie 100 materials testing machine with a 500 N load cell (Fig. 1). Adhesive force was the force required to pull the specimen off a substrate. The euthanized fish were attached to the moving cross-head of the MTS with fishing line or suture thread looped through the body of the fish above and around the adhesive disc. Substrate containers were mounted to the base of the MTS and filled with enough seawater to cover the specimens. Prior to each test, we pressed down on the fish to evacuate water under the disc and ensure adhesion. Each fish was preconditioned with three tests that were discarded. A random substrate was selected and five tests were completed. This was repeated until the individual was tested on each of the substrates. All tests were conducted with the cross-head of the MTS moving at 1 m min<sup>-1</sup> and force was continually recorded at 500 Hz.

Only the maximum recorded force for each substrate–specimen pair was used in this analysis. Peak forces were determined from the force–extension curves as the highest recorded load prior to a sudden drop, which indicated fish detachment (Fig. 2). Our data were combined with published northern clingfish suction data

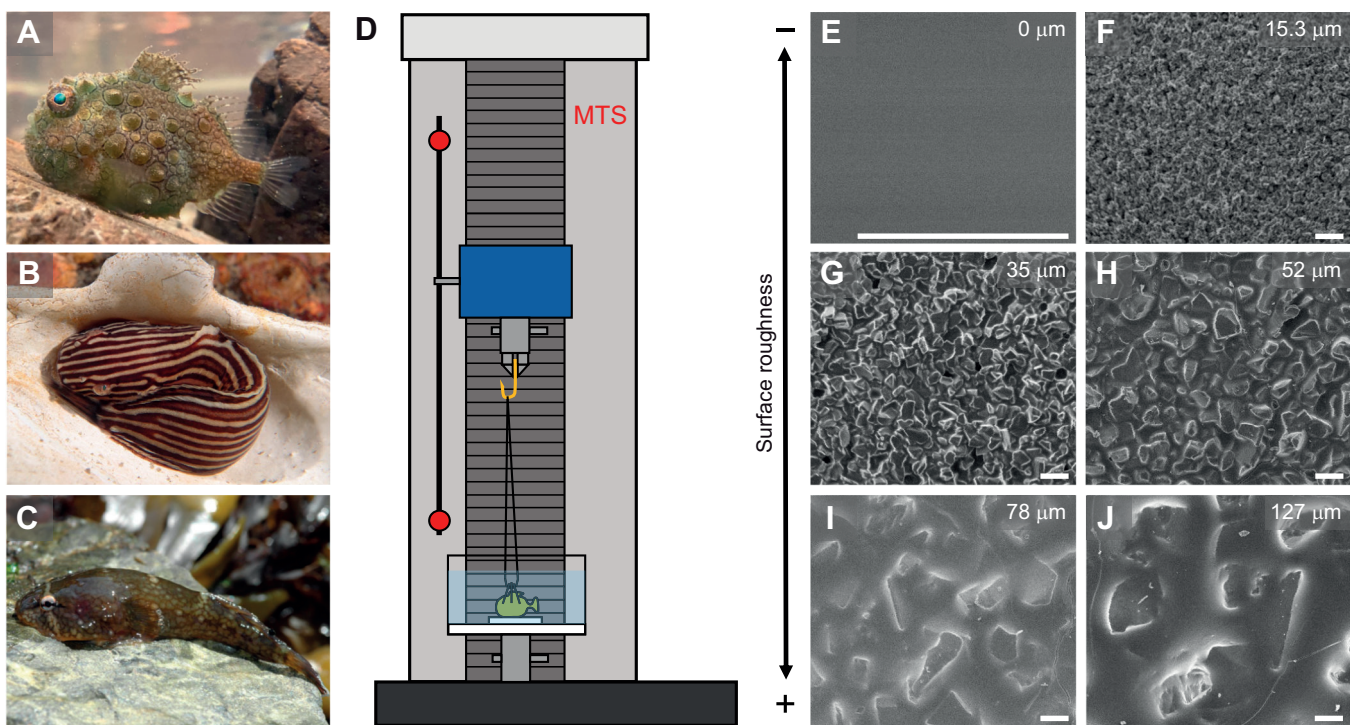


**Fig. 1. Images of the animals and experimental set up used in this study.** (A–C) Live photos of the Pacific spiny lumpsucker (A), marbled snailfish (photo provided by Jim Auzins, Jim Auzins Photography; B) and northern clingfish (photo provided by Thomas Kleinteich, TPW Prüfzentrum GmbH; C). (D) Schematic diagram of the testing set up used to measure the suction forces of each fish (modified from figshare: <https://doi.org/10.6084/m9.figshare.19586668.v2>). (E–J) Scanning electron micrographs showing the increasing roughness of the six surfaces the fish were tested on (average particle size is given in each image). Scale bars: 100 μm.

( $n=21$ , SL 7.0–12 cm, BM 8.2–42.0 g) on surfaces of the same roughness values (Wainwright et al., 2013). Because adhesive forces are dependent on disc size, which varies with body size and between species, we normalized peak force by dividing by body weight. Peak tensile stress ( $P_{ad}$ ) was calculated as a function of adhesive force ( $F_{ad}$ ) over disc area ( $A$ ) as follows:

$$P_{ad} = \frac{F_{ad}}{A}. \quad (1)$$

To further characterize adhesive performance, we also compared the amount of work required to dislodge each fish. Because the specimens were attached to the MTS with a variable amount of slack, we needed to standardize the force–extension curves. For each trial, we set the zero extension point to be where the load increased 0.1 N over a baseline. The baseline was calculated by averaging 15 points gathered before slack was taken up on the attachment string. The amount of work required to dislodge each fish was measured as the area under the force–extension curve from zero extension to the extension at peak force (Fig. 2). Data from the adhesive tests and force–extension curves are present in Tables S1 and S2, respectively.

### Comparing disc morphology

To investigate potential morphological correlates of adhesive performance, we compared the morphology of clingfish, lumpsucker and snailfish adhesive discs using micro-computed tomography (micro-CT) and scanning electron microscopy (SEM). We used micro-CT scanning to examine the morphology of the bony supports in the discs (the pelvic girdles). Available scans of the northern clingfish, Pacific spiny lumpsucker and marbled snailfish were downloaded from the online repository MorphoSource and

supplemental scans were generated to obtain at least five individual scans per species. These scans were uploaded to MorphoSource (<https://www.morphosource.org/>; see Table S3). Preserved specimens of clingfish and snailfish on loan from the University of Washington Fish Collection were scanned at the Friday Harbor

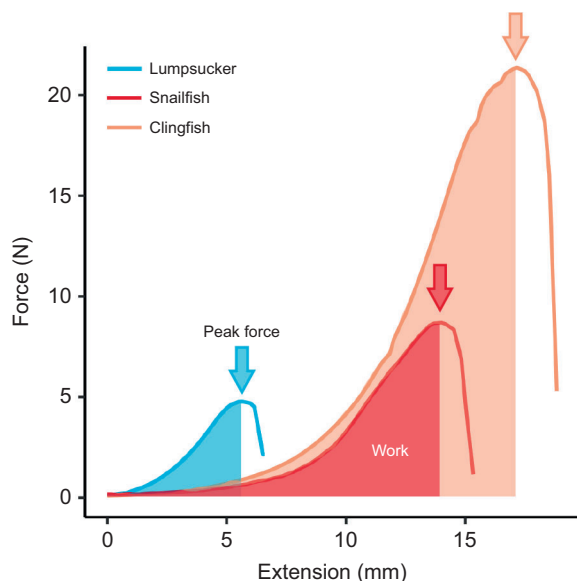


**Fig. 2. Example force–extension curves from the pull-off trials.** Peak adhesive forces were measured as the highest recorded force prior to disc failure, indicated by the arrows. Work to detachment was measured as the area under each force–extension curve from zero extension to failure, indicated by the shaded regions.

Laboratories Karel F. Liem Bio-imaging Center using a Bruker Skyscan 1173. Scanning was conducted with a voxel size of 29.8  $\mu\text{m}$ , a voltage of 65 kV, an amperage of 123  $\mu\text{A}$ , and an exposure time of 1.175 s. We used the open-source bioimaging platform 3D Slicer and the SlicerMorph toolkit to segment, visualize and measure several aspects of the discs (Kikinis et al., 2014; Rolfe et al., 2021). There are no known osteological traits linked to suction performance (Palecek et al., 2022), so we focused on identifying characteristics that differentiated the discs. From each disc, we measured (1) the length, (2) the width and (3) the height of the pelvic girdle, (4) the average length of the fin rays, (5) the average spacing between the base of the fin rays on the left side and (6) the average distance between corresponding fin rays on the contralateral side.

We used SEM to compare the surface morphology and microstructures of the adhesive discs. Adhesive discs for three specimens per species were carefully dissected away from the body and fixed in a 10% buffered formaldehyde solution. Once fully fixed, adhesive discs were transferred through an ethanol dehydration series to 100% ethanol. Tissue was then dried using a critical point dryer (Samdri 790, Tousimis Research Corp.). Once dried, tissue samples were sputter coated with a Cressington 108 Sputter Coater (Ted Pella, Inc.) with gold palladium, and imaged with a JEOL Neoscope JCM-5000.

### Statistical analyses

All statistical analyses were performed in R version 4.0.2 (<http://www.R-project.org/>) and the scripts are provided in the Supplementary Materials and Methods. We used linear mixed-effect models (LMMs) to compare the peak force, force times body

weight, stress and work between species on the different surfaces. The LMMs were performed with random intercepts and fitted using restricted maximum likelihood in the *lme4* R package (Bates et al., 2015). Species and surface roughness (and their interaction) were included as fixed effects, and individual specimen number as the random effect to account for repeated measures [ $\gamma \sim \text{Species} * \text{Surface Roughness} + (1|\text{Individual})$ ]. To calculate the estimated marginal means of the fixed effects, standard error and confidence intervals on each substrate, we used the *emmeans* R package (<https://CRAN.R-project.org/package=emmeans>). The coefficient of determination or goodness-of-fit of each model was calculated as Nagakawa's marginal  $R^2$  ( $R^2_{\text{marg}}$ , which describes the amount of variation explained by only the fixed effects) and conditional  $R^2$  ( $R^2_{\text{cond}}$ , which describes the amount of variation explained by both the fixed and random effects), using the *performance* R package (<https://CRAN.R-project.org/package=performance>). If  $R^2_{\text{cond}}$  is higher than  $R^2_{\text{marg}}$ , the individual variation has a non-zero effect on the measured performance variables.

We also investigated how adhesive disc area ( $\text{cm}^2$ ), suction forces (N) and work (mJ) scaled with body mass (g) over ontogeny, as well as how force scaled with disc area. Reduced major axis (RMA) regressions were performed on  $\log_{10}$ -transformed morphometric and performance data using the *lmodel2* R package (<https://CRAN.R-project.org/package=lmodel2>). RMA regression models were used because they account for potential measurement error in both variables, but also remain the least sensitive to assumptions about error structure in the data than other model II regressions (LaBarbera, 1989). We compared the regression slopes with their predicted slopes assuming isometric growth. Because force is often

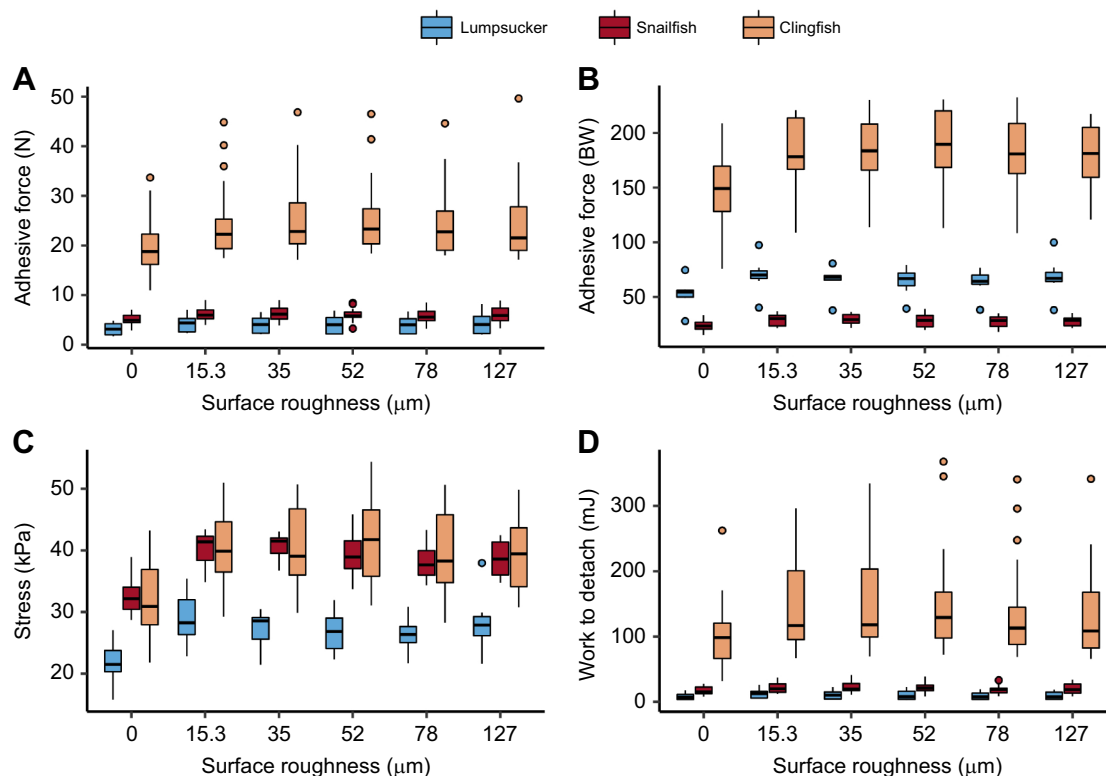


**Fig. 3. Variation in the adhesive performance of the Pacific spiny lumpsucker, marbled snailfish and northern clingfish.** Comparison of (A) adhesive force, (B) normalized adhesive force per body weight (BW), (C) tensile stress and (D) work to detach for the Pacific spiny lumpsucker ( $n=7$ ; blue), marbled snailfish ( $n=12$ ; red) and northern clingfish ( $n=21$ ; orange) on six surfaces of different roughness. Boxplots show the median, upper and lower quartiles, interquartile range and outliers as determined by the 1.5 interquartile rule (circles).

proportional to the cross-sectional area of muscle, the predicted isometric slope for both force and disc area relative to mass was 0.66, and the slope for work (force $\times$ distance) was 1. The predicted slope for force versus disc area was also 1. Scaling relationships were considered allometric if the predicted slopes for isometry fell outside the 95% confidence interval of the calculated RMA regression slopes. Our data and the literature show no significant variation in adhesive performance across rough surfaces, so for the scaling analysis we pooled data from all the rough surfaces.

To identify which, if any, of the morphological traits we measured from the micro-CT scans could be used to differentiate species, we used a discriminant function analysis (DFA). First, we log<sub>10</sub>-transformed all of the traits and then regressed the measurements against pelvic girdle length. The residuals were used as size-corrected variables in the DFA, performed with the MASS package in R (<https://CRAN.R-project.org/package=MASS>).

## RESULTS

### Adhesive performance

Pacific spiny lumpsuckers and marbled snailfish generated similar peak adhesive forces that were considerably lower than the forces of the northern clingfish ( $R^2_{\text{marg}}=0.747$ ,  $R^2_{\text{cond}}=0.987$ ) (Fig. 3A, Table 1). Each species adhered better on the rough surfaces than on the smoothest one, but generally adhered equally well across all rough surfaces (Table 1). Lumpsucker forces ranged between 2.0 and 8.2 N on rough surfaces, and were ~24% lower on the smoothest surface. Snailfish forces were between 3.2 and 9.0 N on

rough surfaces, and were ~17% lower on the smoothest surface. Clingfish forces were between 17.1 and 49.6 N on rough surfaces, and were ~20% lower on the smoothest surface.

Clingfish generated the greatest normalized adhesive force followed by the lumpsuckers and then snailfish ( $R^2_{\text{marg}}=0.883$ ,  $R^2_{\text{cond}}=0.998$ ) (Fig. 3B, Table 1). Clingfish adhesive forces varied between 76 and 232 times their body weight. The forces of lumpsucker adhesion varied between 28 and 100 times their body weight, whereas snailfish adhesion was half that and ranged between 15 and 39 times their body weight. By contrast, the tensile stress on snailfish and clingfish adhesive discs was similar, and ~50% higher than the stress on lumpsucker discs ( $R^2_{\text{marg}}=0.523$ ,  $R^2_{\text{cond}}=0.908$ ) (Fig. 3C; Table 1). The stress varied between 29 and 46 kPa for snailfish discs, and between 22 and 54 kPa for clingfish discs. Stress on lumpsucker discs only ranged between 16 and 38 kPa. Lumpsuckers had better whole-body performance than the snailfish (higher mass-normalized adhesive forces), but snailfish adhesive discs outperformed lumpsucker discs in tensile stress.

The work required to remove each species showed similar patterns to peak adhesive force. Lumpsuckers and snailfish required relatively similar, low amounts of work to be detached, while clingfish required substantially more ( $R^2_{\text{marg}}=0.573$ ,  $R^2_{\text{cond}}=0.945$ ) (Fig. 3D, Table 1). Each species also required more work on rougher surfaces than on the smooth one. Lumpsuckers required between 3.0 and 25.8 mJ of work to be detached from the rough surfaces, and ~21% less on the smoothest surface. Snailfish required between 8.0 and 41.0 mJ of work on the rough surfaces and ~23% less on the

**Table 1. Comparison of peak force, force per body weight, stress and work to detach for the Pacific spiny lumpsucker, marbled snailfish and northern clingfish on six surfaces that varied in roughness**

	Lumpsucker (n=7)		Snailfish (n=12)		Clingfish (n=21)		$R^2_{\text{marg}}$	$R^2_{\text{cond}}$
	FE $\pm$ s.e.	95% CI	FE $\pm$ s.e.	95% CI	FE $\pm$ s.e.	95% CI		
Force (N)							0.747	0.987
0	3.15 $\pm$ 2.13	−1.16, 7.45	5.02 $\pm$ 1.63	1.73, 8.31	20.01 $\pm$ 1.23	17.52, 22.50		
15.3	4.21 $\pm$ 2.13	−0.10, 8.51	6.20 $\pm$ 1.63	2.91, 9.49	24.84 $\pm$ 1.23	22.35, 27.33		
35	4.01 $\pm$ 2.13	−0.30, 8.32	6.29 $\pm$ 1.63	3.00, 9.58	25.55 $\pm$ 1.23	23.06, 28.04		
52	4.01 $\pm$ 2.13	−0.30, 8.32	6.00 $\pm$ 1.63	2.71, 9.29	25.77 $\pm$ 1.23	23.28, 28.25		
78	3.93 $\pm$ 2.13	−0.38, 8.24	5.86 $\pm$ 1.63	2.56, 9.16	24.86 $\pm$ 1.23	22.37, 27.34		
127	4.32 $\pm$ 2.13	0.01, 8.63	6.03 $\pm$ 1.63	2.74, 9.32	24.78 $\pm$ 1.23	22.29, 27.27		
Force (BW)							0.883	0.998
0	52.6 $\pm$ 9.57	33.3, 71.9	23.5 $\pm$ 7.31	8.8, 38.2	145.1 $\pm$ 5.52	133.9, 156.2		
15.3	69.8 $\pm$ 9.57	50.5, 89.1	29.0 $\pm$ 7.31	14.3, 43.7	180.3 $\pm$ 5.52	169.2, 191.5		
35	65.1 $\pm$ 9.57	45.8, 84.4	29.3 $\pm$ 7.31	14.5, 44.0	184.4 $\pm$ 5.52	173.2, 195.5		
52	64.1 $\pm$ 9.57	44.8, 83.4	28.2 $\pm$ 7.31	13.5, 42.9	187.1 $\pm$ 5.52	176.0, 198.3		
78	63.1 $\pm$ 9.57	43.8, 82.4	27.4 $\pm$ 7.35	12.6, 42.2	180.2 $\pm$ 5.52	169.1, 191.3		
127	68.3 $\pm$ 9.57	49.0, 87.6	27.7 $\pm$ 7.31	13.0, 42.4	178.5 $\pm$ 5.52	167.4, 189.7		
Stress (kPa)							0.523	0.908
0	21.8 $\pm$ 1.96	17.8, 25.7	32.6 $\pm$ 1.50	29.6, 35.6	32.0 $\pm$ 1.13	29.7, 34.3		
15.3	29.0 $\pm$ 1.96	25.1, 33.0	40.3 $\pm$ 1.50	37.3, 43.3	39.8 $\pm$ 1.13	37.5, 42.1		
35	27.1 $\pm$ 1.96	23.2, 31.1	40.8 $\pm$ 1.50	37.8, 43.8	40.8 $\pm$ 1.13	38.5, 43.0		
52	26.8 $\pm$ 1.96	22.8, 30.7	39.1 $\pm$ 1.50	36.1, 42.1	41.3 $\pm$ 1.13	39.0, 43.6		
78	26.3 $\pm$ 1.96	22.4, 30.3	38.0 $\pm$ 1.52	35.0, 41.1	39.8 $\pm$ 1.13	37.6, 42.1		
127	28.3 $\pm$ 1.96	24.4, 32.3	38.7 $\pm$ 1.50	35.7, 41.7	39.4 $\pm$ 1.13	37.2, 41.7		
Work (mJ)							0.573	0.945
0	8.2 $\pm$ 20.1	−32.2, 48.6	16.4 $\pm$ 15.3	−14.5, 47.2	103.6 $\pm$ 11.6	80.2, 126.9		
15.3	12.4 $\pm$ 20.1	−28.1, 52.8	21.8 $\pm$ 15.3	−9.1, 52.6	143.2 $\pm$ 11.6	119.9, 166.6		
35	10.7 $\pm$ 20.1	−29.7, 51.1	23.1 $\pm$ 15.3	−7.8, 54.0	149.7 $\pm$ 11.6	126.3, 173.0		
52	10.5 $\pm$ 20.1	−29.9, 50.9	22.2 $\pm$ 15.3	−8.6, 53.1	152.3 $\pm$ 11.6	129.0, 175.6		
78	9.2 $\pm$ 20.1	−31.2, 49.6	19.2 $\pm$ 15.4	−11.8, 50.3	141.2 $\pm$ 11.6	117.9, 164.6		
127	9.6 $\pm$ 20.1	−30.9, 50.0	19.9 $\pm$ 15.3	−11, 50.7	132.8 $\pm$ 11.6	109.4, 156.1		

Statistical analyses (linear mixed-effects models) were performed based on the model: lmer(y~Substrate stiffness \* Surface roughness+(1|Individual)). The fixed effects (FE), standard error (s.e.) and 95% confidence intervals (CI) were estimated with the emmeans R package. The goodness-of-fit of each model was calculated as Nagakawa's  $R^2$  values using the performance R package:  $R^2_{\text{marg}}$  represents the variance explained by only the fixed effects;  $R^2_{\text{cond}}$  represents the variance explained by the fixed and random effects.

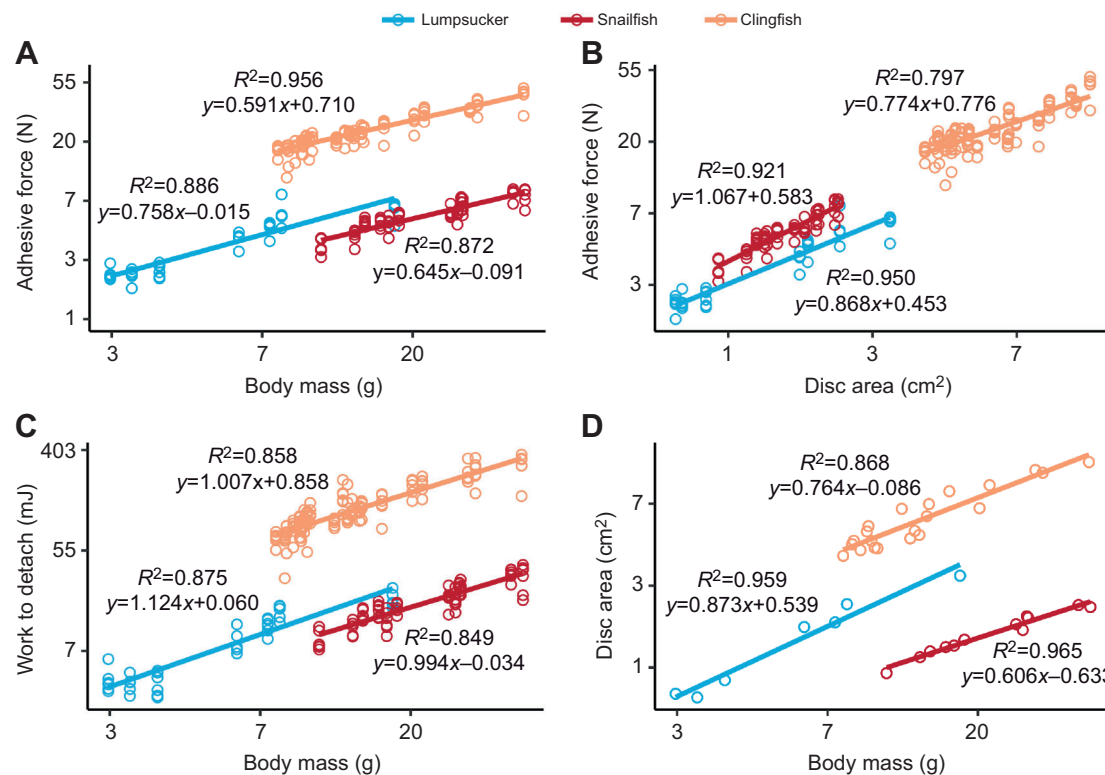


**Fig. 4. Scaling relationships of different performance and trait values.** Reduced major axis (RMA) regressions between (A) adhesive force over body mass, (B) adhesive force over disc area, (C) work to detach over body mass and (D) disc area over body mass. The force and work data collected from the five non-zero roughness surfaces were pooled for each graph. The colored lines show the calculated RMA regression line for each species. See Table 2 for more details on the RMA results.

smoothest one. Clingfish required between 65.9 and 367.8 mJ of work on the rough surfaces and ~28% less on the smoothest one.

#### Allometry of adhesion

Adhesive performance was positively correlated with body mass for all species (Fig. 4, Table 2). Over ontogeny, adhesive force scaled isometrically with mass for snailfish (slope=0.645), with positive allometry for lumpsuckers (slope=0.758) and with negative allometry for clingfish (slope=0.591) (Fig. 4A, Table 2). With disc area, adhesive forces scaled with negative allometry for lumpsuckers (slope=0.868) and clingfish (slope=0.774), but isometrically for snailfish (slope=1.067) (Fig. 4B, Table 2). This

indicates that peak stress decreases as clingfish and lumpsuckers get larger, but remains constant across snailfish ontogeny. The work required to detach the fishes scaled isometrically for lumpsuckers (slope=1.124), snailfish (slope=0.994) and clingfish (slope=1.007) (Fig. 4C, Table 2).

#### Disc morphology

Adhesive disc area scaled isometrically with body mass for snailfish (slope=0.606) and clingfish (slope=0.764), but with positive allometry for lumpsuckers (slope=0.873) (Fig. 4D, Table 2). Marbled snailfish disc area varied between 0.9 and 2.1 cm<sup>2</sup>. Lumpsuckers had similarly sized discs to the snailfish, ranging

**Table 2. Results from the reduced major axis regressions with suction force, work and disc area (DA) over body mass, as well as force over disc area**

Variable	Species	R <sup>2</sup>	Intercept	Intercept 95% CI	Slope	Slope 95% CI	Expected Isometry Slope	Allometry
Force versus mass	Lumpsucker	0.886	-0.015	-0.088, 0.051	0.758	0.673, 0.854	0.66	P
	Snailfish	0.872	-0.091	0.176, -0.013	0.645	0.587, 0.709	0.66	I
	Clingfish	0.956	0.710	0.681, 0.737	0.591	0.567, 0.616	0.66	N
Force versus DA	Lumpsucker	0.950	0.453	0.444, 0.461	0.868	0.802, 0.939	1	N
	Snailfish	0.921	0.583	0.569, 0.596	1.067	0.990, 1.149	1	I
	Clingfish	0.797	0.776	0.720, 0.827	0.774	0.709, 0.845	1	N
Work versus mass	Lumpsucker	0.875	0.060	-0.055, 0.161	1.124	0.992, 1.274	1	I
	Snailfish	0.849	-0.034	-0.177, 0.096	0.994	0.897, 1.102	1	I
	Clingfish	0.858	0.961	0.873, 1.042	1.007	0.936, 1.084	1	I
DA versus mass	Lumpsucker	0.959	-0.539	-0.711, -0.401	0.873	0.694, 1.099	0.66	P
	Snailfish	0.965	-0.633	-0.746, -0.534	0.606	0.532, 0.691	0.66	I
	Clingfish	0.868	-0.086	-0.251, 0.053	0.764	0.642, 0.909	0.66	I

The allometry column indicates whether a trait shows a pattern of isometric growth (I), negative allometry (N) or positive allometry (P). A scaling relationship was considered allometric if the expected isometry slope for isometry fell outside the 95% confidence interval.

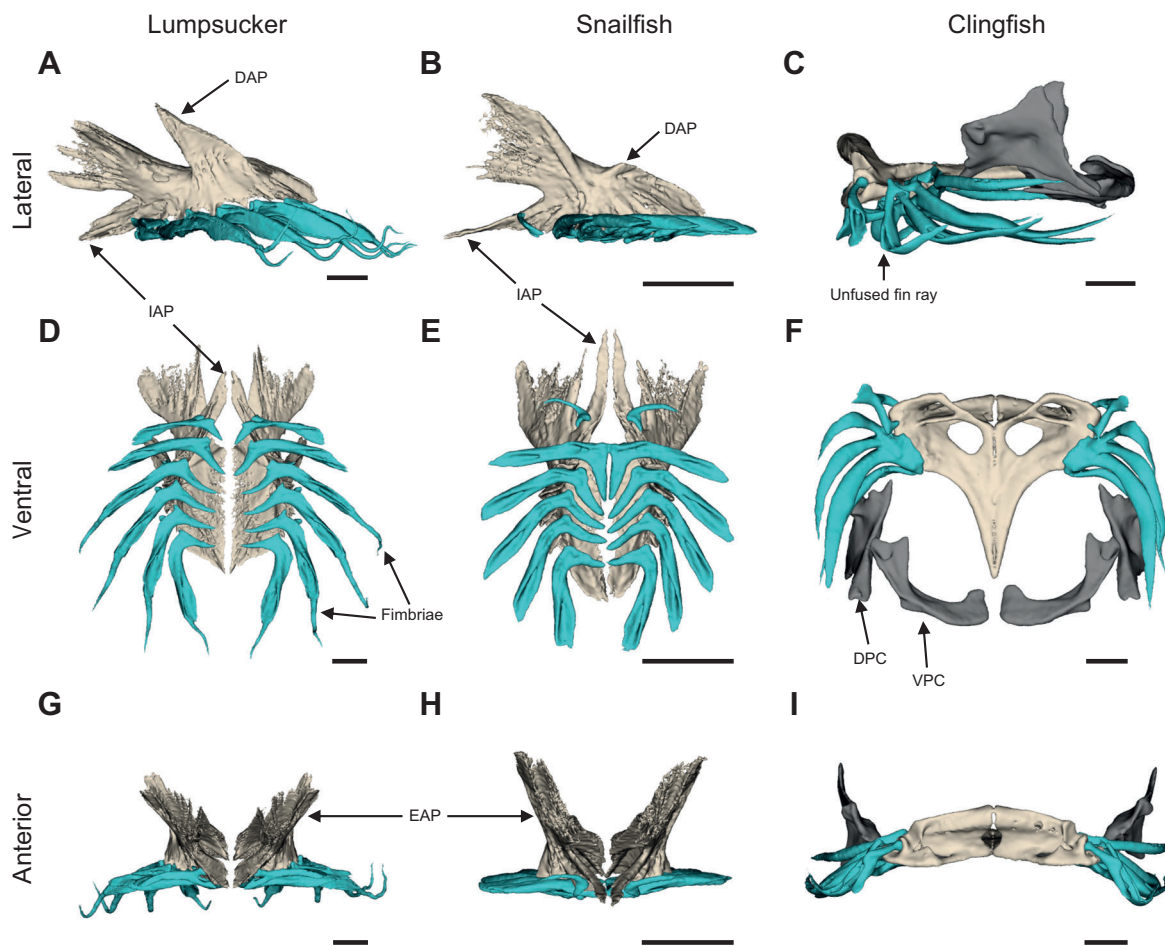


**Fig. 5. Models of the bones in the ventral adhesive discs of the Pacific spiny lumpsucker, marbled snailfish and northern clingfish.** The discs are shown from a left-facing lateral view (A–C), ventral view (D–F) and anterior view (G–I) for each species. All three adhesive discs are supported by a pelvic girdle (beige) and pelvic fin rays (blue), but the clingfish disc is also supported by elements from the pectoral girdle that have migrated posteriorly (gray). DAP, dorsal ascending process; DPC, dorsal postcleithrum; EAP, external ascending process; IAP, inferior ascending process; VPC, ventral postcleithrum. Scale bars: 2.5 mm.

between 0.7 and 3.1 cm<sup>2</sup> in area, but their discs were much larger relative to their body size. The clingfish had the largest discs, ranging between 3.9 and 12.3 cm<sup>2</sup> in area.

Although outwardly similar, lumpsucker and snailfish disc morphology varied in the size and placement of fin rays (Figs 5, 6). The first pair of snailfish pelvic fin rays were highly reduced, while the last five were more robust and located closer together near the midline of the disc. By contrast, lumpsucker fin rays were all of relatively similar size, more spaced apart and further from the midline. Lumpsucker fin rays were generally more robust than those of snailfish, but the distal ends of the last four rays were more filamentous and segmented (Fig. 5). Lumpsuckers and snailfish had relatively elliptical pelvic girdles (from the ventral perspective) but they differed in the size of their anterior and dorsal processes. Lumpsuckers had more pronounced dorsal ascending processes (DAP), while the snailfish had longer internal ascending processes (IAP) on the anterior side of the pelvic girdle (Fig. 5). In clingfish, the pelvic girdle resembled a wide, flat triangle. Most fin rays were large, but not fused, and formed the lateral margins of the disc (Fig. 5). Meanwhile the dorsal and ventral postcleithrum, bony elements from the pectoral girdle, formed the caudal margin of the disc (Fig. 5). The DFA showed height and width of the pelvic girdle, along with the average spacing between neighboring fin rays were

the best traits for distinguishing between the discs of the three species (Fig. S1).

Lumpsucker, snailfish and clingfish adhesive discs were covered in soft papillae of variable sizes that formed a ring around the disc, and none of the papillae extended to the edge or covered the center (Fig. 6G–I). Clingfish papillae were smaller and more numerous than the papillae on either the snailfish or lumpsucker. They were compact and left little space between them. Lumpsuckers and snailfish had larger papillae that were interspersed with smaller papillae and were nearly symmetrical between the left and right sides of the disc. All papillae were composed of smaller villi, making them highly deformable surfaces. Like the lumpsucker papillae, clingfish and snailfish papillae also fluoresce when exposed to royal blue light (440–460 nm; Fig. 6D–F).

## DISCUSSION

Clingfish, lumpsuckers and snailfish are all capable of adhering to a variety of rough surfaces, but clingfish adhesive performance was greater than that of lumpsuckers or snailfish. Our findings support our prediction that species living in habitats with stronger and more variable flow regimes should generate higher adhesive forces. With their impressive pull-off forces (76–232 times their body weight), the northern clingfish lives in the most

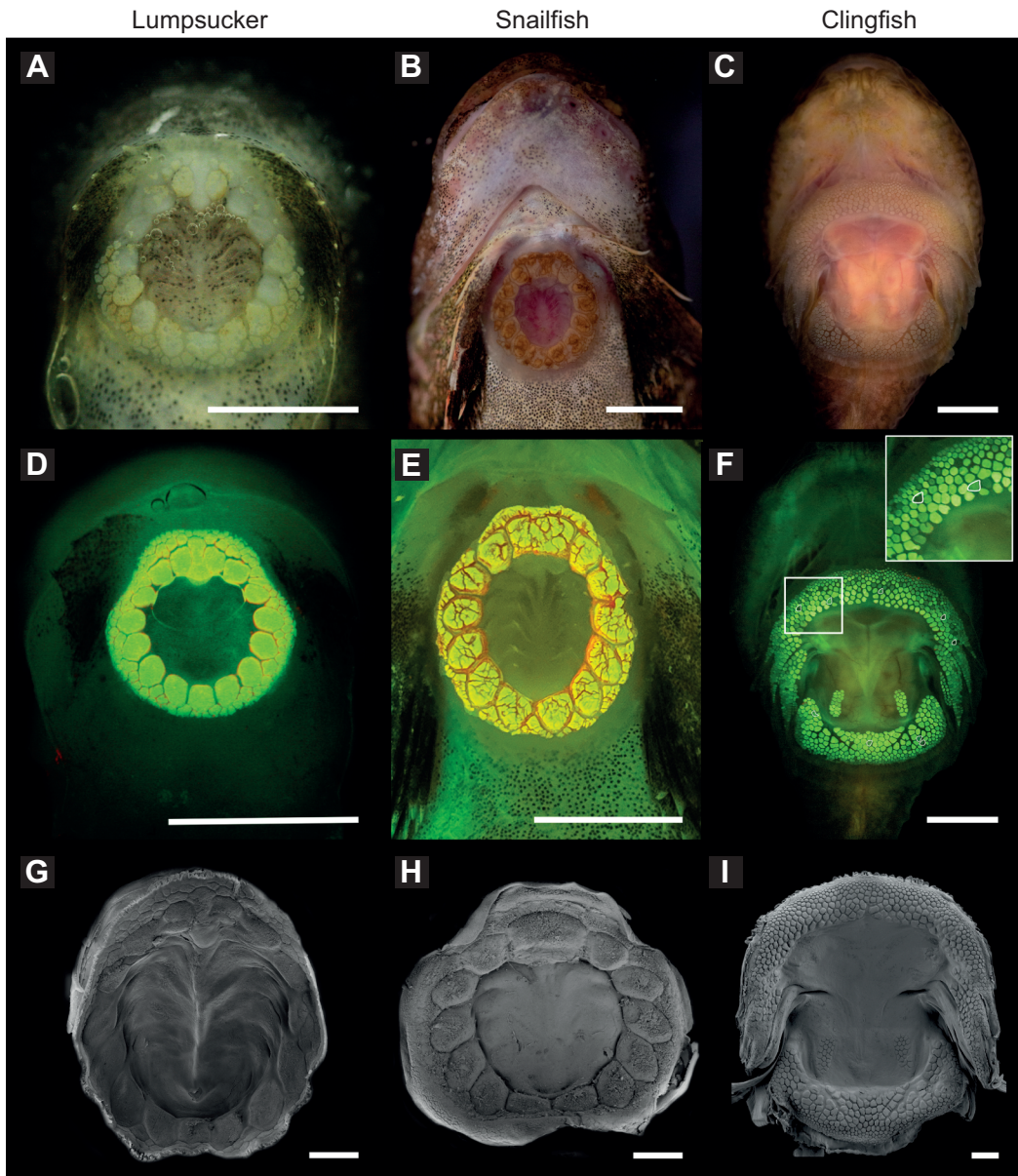


**Fig. 6. Visualizations of the ventral adhesive discs of the Pacific spiny lumpsucker, marbled snailfish and northern clingfish.** (A–C) Photos of adhesive discs from live fish showing the relative size of discs. (D–F) The papillae of all three discs fluoresce when illuminated by royal blue light (440–460 nm). The boxed region in F is shown on an expanded scale in the inset. Scale bars in A–F: 1 cm. (G–I) Scanning electron microscopy images of the discs as a series of composites. Scale bars in G–I: 100  $\mu$ m.

intense and unpredictable environment of the three species (Wainwright et al., 2013; Ditsche et al., 2014). Sticking to rocks in the wave-swept intertidal zone, clingfish not only have to resist being dislodged by high flow speeds but also have to stick well enough to anchor the body while feeding on an archetypal attached mollusk – the limpet (Wainwright, 2011; Michel, 2013). We know less about the ecology of the Pacific spiny lumpsucker and marbled snailfish, but these species live in deeper subtidal environments, where ocean currents are slower and less variable, generating less lift and drag on these fishes (Holbrook, 1980; Ditsche et al., 2017). A similar line of reasoning might also explain why lumpsucker adhesive forces (28–100 times body weight) are higher than those of the snailfish (15–39 times body weight). Near San Juan Island where the specimens in our study are from, marbled snailfish are only ever caught

in deeper waters near the bottom, whereas Pacific spiny lumpsuckers can be found in deep tidepools or nearshore rocky environments.

The importance of adhesive performance likely changes over ontogeny as the demands of abiotic flows change. Drag forces increase in proportion to cross-sectional area as animals grow, and so we expect suction performance to scale with the square of length or mass $^{2/3}$ . However, snailfish were the only species that showed this scaling relationship for pull-off forces (Fig. 4A, Table 2). The pattern did not change when using different length–mass relationships to predict the body mass of the marbled snailfish. In contrast, clingfish scale with negative allometry, meaning that as they get bigger they produce proportionally lower peak forces (Fig. 4A, Table 2). Perhaps drivers of adhesive performance become more relaxed over the course of clingfish ontogeny, requiring

proportionally less stress as they get bigger. If clingfish are exposed to lower velocity flows as they age, adopt a more streamlined posture or attach to lower rugosity surfaces, adult adhesive force would be less important than in smaller animals. Meanwhile, lumpsucker adhesive forces scale with positive allometry, i.e. they produce proportionally higher forces as they get bigger, which is likely an adaptation for the consequences of their drag-inducing body shape. Lumpsuckers are rotund, which is certainly high drag relative to the usual fusiform body plan of fishes. As they grow, they develop spiky armor that should lead to even higher drag than their portly profile would imply. The conical odontodes covering lumpsucker bodies get larger and more numerous, which in turn gives the fish a more pronounced bulbous appearance as they grow (Woodruff et al., 2022). It is noteworthy that the work to detach a fish (regardless of species) scales isometrically with mass. We propose no reason for this, but it suggests a decoupling of peak force and work. Perhaps work to detach will become more informative when varying the pull-off speed (Anderson and Kawano, 2022).

There is clearly more than one strategy for increasing adhesive performance. While snailfish generate the lowest forces relative to body weight, their peak stress is as high as in clingfish. In contrast, lumpsuckers generate lower stress – their discs are less capable of generating adhesive force. Lumpsucker discs generate even lower stress with increasing size, but they have proportionally bigger discs as they grow. The larger discs compensate for the less effective morphology, so there may be varying selective pressures acting on different aspects of performance. Both relative disc size and disc morphology are labile traits that vary across the clingfish, lumpsucker and snailfish phylogenies (Orr et al., 2019; Conway et al., 2020; Voskoboinikova et al., 2020). We have shown the performance of discs has several axes of variation as well, and comparing performance within these families would be fruitful. It is in this context that we would expect to be able to unravel the complex relationship between morphology and performance.

Snailfish discs outperform similarly sized lumpsucker discs despite having a similar appearance and shared common ancestry. However, beneath the soft tissue there are differences in the underlying skeleton (modified pelvic girdle and fin rays) (Fig. 5). Experiments using bioinspired suction cups have shown mixed results as to whether the internal support structures are significant contributors to suction performance (Ditsche et al., 2016; Palecek et al., 2021b, 2022). We propose that the skeletal elements of the snailfish disc provide stiffer support that prevents premature failure compared with that of lumpsuckers. The supporting skeleton of a snailfish disc is compact, with stout fin rays closely arrayed at the center of the disc. In contrast, the fin rays of the lumpsucker disc are further from the midline, and taper into fine fimbriae at the edge – an arrangement that appears to be less stiff than that of the snailfish. We look to the details of our detachment test for some support of this hypothesis. The slopes of the linear region of the force–extension curves, which were converted into stress–strain curves to ameliorate the effects of body size, are steeper in the snailfish than in the lumpsucker, which implies, in some sense, that the snailfish disc is stiffer (Fig. S2). By this notion of stiffness, snailfish ( $92.4 \pm 2.03$  kPa) have twice the resistance to strain that lumpsuckers do ( $47.9 \pm 1.31$  kPa). Formal investigations on the material properties of the pelvic girdles and fin rays of lumpsucker and snailfish, as well as those of clingfish, may provide better insight on their function during adhesion (Taft and Taft, 2012; Taft et al., 2017; Aiello et al., 2018).

Here, we measured two performance metrics for three lineages of sticky fishes over ontogeny, and unsurprisingly found variation. We

wonder whether this variation appropriately reflects the lives that these fishes lead, because under any fixed set of test conditions, variation is to be expected. Relevant tests should take the ecological reality of the fishes into account and challenge them with forces (magnitude and direction) that mimic those dealt with in nature (Higham et al., 2021). While pulling these fishes off a substrate at a relatively low rate of strain is a good way to assess the capabilities of the ‘machine’ that powers attachment, we suspect that it is a poor way to capture their actual day to day performance. Furthermore, the fishes were tested in tension to be comparable with previous clingfish studies, but these fishes are far more likely to experience shear forces in the ocean. We would like to see the attachment force measurements of clingfish, lumpsuckers and snailfish move in the direction of the work done on waterfall-climbing gobies, where the natural challenge to adhesion is well captured by the experimental design (Christy and Maie, 2019; Maie and Blob, 2021; Maie, 2022). When combined with standardized pull-off tests, ecologically informed experiments would provide complementary insight into the diversity of the realized performance space of these fishes in response to the abiotic loads in their natural environments.

#### Acknowledgements

We thank the crews of the *R/V Centennial* and the *R/V Kittiwake* at Friday Harbor Laboratories for their assistance in collecting the live snailfish specimens. We thank Katherine Maslenikov (UW) for providing access to preserved specimens for CT scanning. We thank the Karel F. Liem Bio-imaging Center for providing free access to the CT scanner.

#### Competing interests

The authors declare no competing or financial interests.

#### Author contributions

Conceptualization: J.M.H., K.E.C.; Methodology: J.M.H., D.K.W., A.P.S., K.E.C.; Formal analysis: J.M.H.; Investigation: J.M.H., D.K.W., K.E.C.; Resources: A.P.S.; Data curation: J.M.H., D.K.W.; Writing - original draft: J.M.H., D.K.W., K.E.C.; Writing - review & editing: J.M.H., D.K.W., A.P.S., K.E.C.; Visualization: J.M.H., K.E.C.; Funding acquisition: J.M.H., D.K.W., A.P.S., K.E.C.

#### Funding

J.M.H., D.K.W. and A.P.S. were supported by the National Science Foundation (DGE-1746914 to J.M.H.; DBI-1907156 to D.K.W.; DEB-1701665 and DBI-1759637 to A.P.S.). K.E.C. was supported by the Friday Harbor Laboratories (Stephen and Ruth Wainwright Endowment) and the University of Washington (Edwards Award, Wingfield-Ramenofsky Award, and Orians Award). J.M.H., A.P.S., and K.E.C. were also supported by the Seaver Institute.

#### Data availability

All CT scans are uploaded and freely available for download at [www.morphosource.org](http://www.morphosource.org) (see Table S3 for specific links).

#### References

- Aiello, B. R., Hardy, A. R., Cherian, C., Olsen, A. M., Ahn, S. E., Hale, M. E. and Westneat, M. W.** (2018). The relationship between pectoral fin ray stiffness and swimming behavior in Labridae: insights into design, performance and ecology. *J. Exp. Biol.* **221**, jeb163360. doi:10.1242/jeb.163360
- Anderson, P. S. L. and Kawano, S. M.** (2022). Different traits at different rates: the effects of dynamic strain rate on structural traits in biology. *Integr. Comp. Biol.* **62**, 683-699. doi:10.1093/icb/icac066
- Arita, G. S.** (1967). A comparative study of the structure and function of the adhesive apparatus of the Cyclopteridae and Gobiesocidae. Master's thesis, University of British Columbia, Vancouver, Canada.
- Arita, G. S.** (1969). Sexual dimorphism in the cyclopterid fish *Eumicrotremus orbis*. *J. Fish. Res. Board Can.* **26**, 3262-3265. doi:10.1139/f69-312
- Bates, D., Mächler, M., Bolker, B. and Walker, S.** (2015). Fitting linear mixed-effects models using lme4. *J. Stat. Softw.* **67**, 1-48. doi:10.18637/jss.v067.i01
- Bressman, N. R., Armbruster, J. W., Lujan, N. K., Udoeh, I. and Ashley-Ross, M. A.** (2020). Evolutionary optimization of an anatomical suction cup: lip collagen content and its correlation with flow and substrate in neotropical suckermouth catfishes (Loricarioidei). *J. Morphol.* **281**, 676-687. doi:10.1002/jmor.21136

- Budney, L. A. and Hall, B. K.** (2010). Comparative morphology and osteology of pelvic fin-derived midline suckers in lumpfishes, snailfishes and gobies. *J. Appl. Ichthyol.* **26**, 167–175. doi:10.1111/j.1439-0426.2010.01398.x
- Christy, R. M. and Maie, T.** (2019). Adhesive force and endurance during waterfall climbing in an amphidromous gobioid, *Sicyopterus japonicus* (Teleostei: Gobiidae): ontogenetic scaling of novel locomotor performance. *Zoology* **133**, 10–16. doi:10.1016/j.zool.2019.02.001
- Cohen, K. E. and Summers, A. P.** (2022). Dimorphic fluorescence in the pacific spiny lumpucker. *Ichthyol. Herpetol.* **110**, 350–353. doi:10.1643/ji2021019
- Cohen, K. E., Flammang, B. E., Crawford, C. H. and Hernandez, L. P.** (2020a). Knowing when to stick: touch receptors found in the remora adhesive disc. *R. Soc. Open Sci.* **7**, 190990. doi:10.1098/rsos.190990
- Cohen, K. E., Crawford, C. H., Hernandez, L. P., Beckert, M., Nadler, J. H. and Flammang, B. E.** (2020b). Sucker with a fat lip: the soft tissues underlying the viscoelastic grip of remora adhesion. *J. Anat.* **237**, 643–654. doi:10.1111/joa.13227
- Conway, K. W., King, C. D., Summers, A. P., Kim, D., Hastings, P. A., Moore, G. I., Iglesias, S. P., Erdmann, M. V., Baldwin, C. C., Short, G. et al.** (2020). Molecular phylogenetics of the clingfishes (Teleostei: Gobiesocidae)—implications for classification. *Copeia* **108**, 886–906. doi:10.1643/C12020054
- De Meyer, J., Geerinckx, T.** (2014). Using the whole body as a sucker: combining respiration and feeding with an attached lifestyle in hill stream loaches (Balitoridae, Cypriniformes). *J. Morphol.* **275**, 1066–1079. doi:10.1002/jmor.20286
- Ditsche, P. and Summers, A.** (2019). Learning from Northern clingfish (*Gobiesox maeandricus*): bioinspired suction cups attach to rough surfaces. *Philos. Trans. R. Soc. Lond. B Biol. Sci.* **374**, 20190204. doi:10.1098/rstb.2019.0204
- Ditsche, P., Wainwright, D. K. and Summers, A. P.** (2014). Attachment to challenging substrates—fouling, roughness and limits of adhesion in the northern clingfish (*Gobiesox maeandricus*). *J. Exp. Biol.* **217**, 2548–2554. doi:10.1242/jeb.100149
- Ditsche, P., Ford, W. and Summers, A. P.** (2016). The role of cup elasticity in suction attachment in Northern clingfish. *Integr. Comp. Biol.* **56**, e54.
- Ditsche, P., Hicks, M., Truong, L., Linkem, C. and Summers, A.** (2017). From smooth to rough, from water to air: the intertidal habitat of Northern clingfish (*Gobiesox maeandricus*). *Naturwissenschaften* **104**, 33. doi:10.1007/s00114-017-1454-8
- Froese, R., Thorson, J. T. and Reyes, R. B., Jr.** (2014). A Bayesian approach for estimating length-weight relationships in fishes. *J. Appl. Ichthyol.* **30**, 78–85. doi:10.1111/jai.12299
- Fulcher, B. A. and Motta, P. J.** (2006). Suction disk performance of echeneiid fishes. *Can. J. Zool.* **84**, 42–50. doi:10.1139/z05-167
- Gamel, K. M., Garner, A. M. and Flammang, B. E.** (2019). Bioinspired remora adhesive disc offers insight into evolution. *Bioinspir. Biomim.* **14**, 056014. doi:10.1088/1748-3190/ab3895
- Gerringer, M. E., Dias, A. S., Von Hagel, A. A., Orr, J. W., Summers, A. P. and Farina, S.** (2021). Habitat influences skeletal morphology and density in the snailfishes (family Liparidae). *Front. Zool.* **18**, 16. doi:10.1186/s12983-021-00399-9
- Higham, T. E., Ferry, L. A., Schmitz, L., Irschick, D. J., Starko, S., Anderson, P. S., Bergmann, P. J., Jamniczky, H. A., Monteiro, L. R., Navon, D. et al.** (2021). Linking ecomechanical models and functional traits to understand phenotypic diversity. *Trends Ecol. Evol.* **36**, 860–873. doi:10.1016/j.tree.2021.05.009
- Holbrook, J.** (1980). *Circulation in the Strait of Juan de Fuca: Recent Oceanographic Observations in the Eastern Basin*. U.S. Department of Commerce, National Oceanic and Atmospheric Administration, Environmental Research Laboratories.
- Huie, J. M. and Summers, A. P.** (2022). The effects of soft and rough substrates on suction-based adhesion. *J. Exp. Biol.* **225**, jeb243773. doi:10.1242/jeb.243773
- Johnson, C. R.** (1969). Contributions to the biology of the showy snailfish, *Liparis pulchellus* (Liparidae). *Copeia* **1969**, 830–835. doi:10.2307/1441806
- Kells, V. A., Rocha, L. A. and Allen, L. G.** (2016). *A Field Guide to Coastal Fishes: From Alaska to California*. Baltimore, MD: Johns Hopkins University Press.
- Kikinis, R., Pieper, S. D. and Vosburgh, K. G.** (2014). 3D slicer: a platform for subject-specific image analysis, visualization, and clinical support. In *Intraoperative Imaging and Image-Guided Therapy* (ed. F. A. Jolesz), pp. 277–289. New York: Springer.
- Kulik, V. V. and Gerasimov, N. N.** (2016). Length-weight and length-length relationships of 11 fish species from the Sea of Okhotsk. *J. Appl. Ichthyol.* **32**, 1326–1328. doi:10.1111/jai.13225
- Labarbera, M.** (1989). Analyzing body size as a factor in ecology and evolution. *Annu. Rev. Ecol. Syst.* **20**, 97–117. doi:10.1146/annurev.es.20.110189.000525
- Lujan, N. K. and Conway, K. W.** (2015). Life in the fast lane: a review of rheophily in freshwater fishes. In *Extremophile Fishes: Ecology, Evolution, and Physiology of Teleosts in Extreme Environments* (ed. R. Riesch, M. Tobler and M. Plath), pp. 107–136. Cham: Springer International Publishing. doi:10.1007/978-3-319-13362-1\_6
- Maie, T.** (2022). Locomotor challenges of waterfall-climbing gobies during transitions between media. *Integr. Comp. Biol.* **62**, 922–933. doi:10.1093/icb/icac078
- Maie, T. and Blob, R. W.** (2021). Adhesive force and endurance of the pelvic sucker across different modes of waterfall-climbing in gobiid fishes: contrasting climbing mechanisms share aspects of ontogenetic change. *Zoology* **149**, 125969. doi:10.1016/j.zool.2021.125969
- Maie, T., Schoenfuss, H. L. and Blob, R. W.** (2012). Performance and scaling of a novel locomotor structure: adhesive capacity of climbing gobiid fishes. *J. Exp. Biol.* **215**, 3925–3936. doi:10.1242/jeb.072967
- Michel, K. B.** (2013). Kinematics and functional morphology of feeding in the Northern clingfish. *Integr. Comp. Biol.* **53**, e334.
- Orr, J. W., Spies, I., Stevenson, D. E., Longo, G. C., Kai, Y., Ghods, S. and Hollowed, M.** (2019). Molecular phylogenetics of snailfishes (Cottoidei: Liparidae) based on MtDNA and RADseq genomic analyses, with comments on selected morphological characters. *Zootaxa* **4642**, 1–79. doi:10.11646/zootaxa.4642.1.1
- Palecek, A. M., Schoenfuss, H. L. and Blob, R. W.** (2021a). Sticking to it: testing passive pull-off forces in waterfall-climbing fishes across challenging substrates. *J. Exp. Biol.* **224**, jeb228718. doi:10.1242/jeb.228718
- Palecek, A. M., Huie, J. M., Cohen, K. E., Donatelli, C. M. and Summers, A. P.** (2021b). Stuck on you: how pelvic girdle morphology influences adhesion. *Integr. Comp. Biol.* **61**, e1221.
- Palecek, A. M., Schoenfuss, H. L. and Blob, R. W.** (2022). Sucker shapes, skeletons and bioinspiration: how hard and soft tissue morphology generates adhesive performance in waterfall climbing goby fishes. *Integr. Comp. Biol.* **62**, 934–944. doi:10.1093/icb/icac094
- Pietsch, T. W. and Orr, J. W.** (2015). Fishes of the Salish Sea; a compilation and distributional analysis. *NOAA Professional Paper NMFS* **18**, 53.
- Rolfe, S., Pieper, S., Porto, A., Diamond, K., Winchester, J., Shan, S., Kirveslahti, H., Boyer, D., Summers, A. and Maga, A. M.** (2021). SlicerMorph: an open and extensible platform to retrieve, visualize and analyse 3D morphology. *Methods Ecol. Evol.* **12**, 1816–1825. doi:10.1111/2041-210X.13669
- Sandoval, J. A., Jadhav, S., Quan, H., Deheyn, D. D. and Tolley, M. T.** (2019). Reversible adhesion to rough surfaces both in and out of water, inspired by the clingfish suction disc. *Bioinspir. Biomim.* **14**, 066016. doi:10.1088/1748-3190/ab47d1
- Sandoval, J. A., Sommers, J., Peddireddy, K. R., Robertson-Anderson, R. M., Tolley, M. T. and Deheyn, D. D.** (2020). Toward bioinspired wet adhesives: lessons from assessing surface structures of the suction disc of intertidal clingfish. *ACS Appl. Mater. Interfaces* **12**, 45460–45475. doi:10.1021/acsm.mi.0c10749
- Schindelin, J., Arganda-Carreras, I., Frise, E., Kaynig, V., Longair, M., Pietzsch, T., Preibisch, S., Rueden, C., Saalfeld, S., Schmid, B. et al.** (2012). Fiji: an open-source platform for biological-image analysis. *Nat. Methods* **9**, 676–682. doi:10.1038/nmeth.2019
- Shi, H., Holbrook, C. M., Cao, Y., Sepúlveda, N. and Tan, X.** (2021). Measurement of suction pressure dynamics of sea lampreys, *Petromyzon marinus*. *PLoS One* **16**, e0247884. doi:10.1371/journal.pone.0247884
- Taft, N. K. and Taft, B. N.** (2012). Functional implications of morphological specializations among the pectoral fin rays of the benthic longhorn sculpin. *J. Exp. Biol.* **215**, 2703–2710. doi:10.1242/jeb.063958
- Taft, N. K., Taft, B. N., Henck, H., Diamond, K. M., Schoenfuss, H. L. and Blob, R. W.** (2017). Comparative morphology and mechanical properties of the lepidotrichia of climbing and non-climbing Hawaiian gobioid fishes. *Cybium* **41**, 107–115.
- Voskoboinikova, O. S., Kudryavtseva, O. Y., Orlov, A. M., Orlova, S. Y., Nazarkin, M. V., Chernova, N. V. and Maznikova, O. A.** (2020). Relationships and evolution of lump suckers of the family Cyclopteridae (Cottoidei). *J. Ichthyol.* **60**, 154–181. doi:10.1134/S0032945220020204
- Wainwright, D. K.** (2011). Functional morphology of northern clingfish feeding on limpets. *Integr. Comp. Biol.* **51**, e262.
- Wainwright, D. K., Kleinteich, T., Kleinteich, A., Gorb, S. N. and Summers, A. P.** (2013). Stick tight: suction adhesion on irregular surfaces in the Northern clingfish. *Biol. Lett.* **9**, 20130234. doi:10.1098/rsbl.2013.0234
- Wang, Y., Yang, X., Chen, Y., Wainwright, D. K., Kenaley, C. P., Gong, Z., Liu, Z., Liu, H., Guan, J., Wang, T. et al.** (2017). A biorobotic adhesive disc for underwater hitchhiking inspired by the remora suckerfish. *Sci. Robot.* **2**, eaan8072. doi:10.1126/scirobotics.aan8072
- Wang, S., Li, L., Sun, W., Wainwright, D., Wang, H., Zhao, W., Chen, B., Chen, Y. and Wen, L.** (2020). Detachment of the remora suckerfish disc: kinematics and a bio-inspired robotic model. *Bioinspir. Biomim.* **15**, 056018. doi:10.1088/1748-3190/ab9418
- Willis, J., De Perera, T. B., Newport, C., Poncelet, G., Sturrock, C. J. and Thomas, A.** (2019). The structure and function of the sucker systems of hill stream loaches. *bioRxiv* 281592. doi:10.1101/281592
- Woodruff, E. C., Huie, J. M., Summers, A. P. and Cohen, K. E.** (2022). Pacific Spiny Lumpucker armor-Development, damage, and defense in the intertidal. *J. Morphol.* **283**, 164–173. doi:10.1002/jmor.21435